PHYSICAL REVIEW B VOLUME 31, NUMBER 6 15 MARCH 1985

Surface phonon dispersion of $c(2\times2)$ S on Ni(100)

S. Lehwald, M. Rocca,* and H. Ibach
Institut für Grenzflächenforschung und Vakuumphysik, Kernforschungsanlage Jülich, Postfach 1913, D-5170 Jülich, West Germany

Talat S. Rahman
Cardwell Hall, Department of Physics, Kansas State University, Manhattan, Kansas 66506

(Received 15 October 1984)

The dispersion of the adsorbate- and substrate-associated modes of the Ni(100) surface covered with a $c(2\times2)$ sulfur overlayer has been measured along the $\overline{\Gamma}-\overline{X}$ direction by inelastic electron scattering. Experimental data are compared to a lattice dynamical model using an analytical Green's-function technique. The optimum fit is obtained when the sulfur atom is placed at 1.45 Å above the nickel layer.

I. INTRODUCTION

The dispersion of surface phonons on clean surfaces and those with adsorbate layers has become amenable to experimental investigations only recently. Currently, two techniques are in use, namely inelastic scattering of He atoms[1–2] and inelastic scattering of electrons.[3–5] The latter is particularly suitable for studies on the dispersion of the modes of ordered overlayers of chemisorbed atoms or molecules.[5] The first system for which the dispersion of adsorbate and substrate surface modes was measured was the Ni(100) surface covered with a $c(2\times2)$ overlayer of oxygen.[4] Theoretical analysis[6] showed that the dispersion curves could be matched to a simple lattice-dynamical model with nearest-neighbor interactions. In order to also achieve a reasonable fit to the dispersion of the Rayleigh mode, it was found necessary to assume that the coupling between the first- and second-layer nickel atoms reduces to ~ 0.3 of the bulk value, whereas on the clean surface this coupling is enhanced to 1.2 times the bulk value. This finding is in agreement with ion-scattering[7] data, suggesting that on the clean surface the distance between the first and second nickel layers is contracted by -0.06 Å, whereas it is relaxed by $+0.09$ Å when the surface is covered with a $c(2\times2)$ overlayer of oxygen. Thus one has several indications that the bonding between the first- and second-layer nickel atoms is reduced as a result of the Ni—O bonds formed on the surface. It should therefore be interesting to pursue this issue further, with other adsorbates on the same surface forming either weaker bonds or even stronger bonds with nickel. An example of the same overlayer with weaker bonding is the $c(2\times2)$ overlayer of sulfur. As with the $c(2\times2)$ O overlayer, the sulfur system has been investigated extensively with low-energy electron diffraction[8] (LEED) and other structural methods such as extended x-ray absorption fine-structure spectroscopy[9] (EXAFS) and photoelectron diffraction.[10–12] According to these studies, sulfur "sits" in the fourfold hollow sites at (approximately) ~ 1.4 Å above the nickel surface plane.

Our choice of the study of the dispersion of the $c(2\times2)$ sulfur overlayer on the Ni(100) surface also stems from the remarkable difference in the behavior of the sulfur and oxygen overlayers on this surface, as is evident from the available vibrational data for sulfur at the $\overline{\Gamma}$ point of the surface Brillouin zone.[13] It is intriguing that, while for oxygen overlayers there is a considerable softening in the frequency of the oxygen—metal stretch mode from the $p(2\times2)$ to the $c(2\times2)$ structure[13,14] which cannot be explained on the basis of the mere difference in the number of overlayer atoms, no such drastic softening of this mode is observed for the case of similar sulfur overlayers. We believe that, in the case of oxygen overlayers, this softening in frequency is related to the change in the coupling between the first- and second-layer nickel atoms in the presence of a $c(2\times2)$ oxygen overlayer. Thus we do not expect a $c(2\times2)$ sulfur overlayer to greatly influence the nickel interlayer coupling.

In this paper we report on the measurement of the adsorbate and substrate dispersion curves and the theoretical analysis accompanying the data. In agreement with what was expected, we indeed find that no reduction in the bonding between the first and second nickel layers is involved. The dispersion curves for the parallel and perpendicular sulfur modes, as well as the substrate surface modes and resonances, can be matched with a simple nearest-neighbor central force field. However, this satisfactory match with the data is obtained only when the sulfur atoms are placed at least 1.45 Å above the surface. Even with a more complex force field, the agreement with the data is not as good if the sulfur atom is allowed to sit any closer to the surface.

The paper is organized as follows. In the next section we give some experimental details with regard to sample preparation and data acquisition. In Sec. III the experimental results are presented. In Sec. IV we briefly describe our theoretical model calculation. In Sec. V we compare the theoretical and experimental results on the dispersion curves of sulfur and nickel modes for different vertical distances of sulfur and different force fields. In Sec. VI we discuss our best-fit vertical distance of sulfur in the light of structure data and with respect to limits of the harmonic approximation.

II. EXPERIMENTAL DETAILS

The Ni single crystal was cleaned by repeated cycles of Ne-ion bombardment and annealing to 1400 K until the crystal was leached of carbon and sulfur, and no traces of either impurity could be detected by our cylindrical-mirror-analyzer (CMA) Auger spectrometer, even after annealing and cooling down to room temperature. In order to obtain the $c(2\times2)$ sulfur layer, we exposed the sample to H_2S with the sample temperature held at 500 K. Exposure was performed using an open-tube dosing system. The amount of H_2S was controlled by a spinning-ball friction gauge. The sulfur-surface coverage saturated after an exposure equivalent to ~ 15 L H_2S (1 L= 1 langmuir= 10^{-6} Torr sec). The saturation corresponded to a peak-to-peak ratio in the Auger spectrum of $I_{S_{152}}/I_{Ni_{848}}=1.0$. A sharp $c(2\times2)$ LEED pattern was observed after this treatment. Under our vacuum conditions of 1×10^{-11} Torr pressure, the sulfur-covered surface remained free of contaminants for long periods of time. Possible trace contaminants of H and CO were flashed-off before each series of measurements.

Electron-energy losses were measured with a double-pass energy-loss spectrometer capable of impact energies variable between 1 and 500 eV. The scattering plane was aligned along with the surface normal and the [110] direction. By appropriate choice of the impact energy E_0, the angle of the incident beam, θ_i, and the angle of the scattered beam, θ_f, the phonon dispersion could be measured for wave vector $\mathbf{Q}_{\parallel}$ varying along the $\bar{\Gamma}-\bar{X}$ ([110]) direction of the surface Brillouin zone (Fig. 1). According to the selection rules in electron-phonon scattering,[15] modes which are even with respect to the mirror plane spanned by the [110] direction and the surface normal (sagittal plane) are observable, while the odd modes are not. This excludes the S_1 mode[16] from contributing to the loss spectra. Theoretical calculations[17] as well as experimental studies[18] show that the inelastic cross section for phonon scattering is a strong, sometimes rapidly varying function of the scattering parameters. Measuring dispersion curves therefore involves a search for optimum scattering cross sections for the individual modes of the system. For any $\mathbf{Q}_{\parallel}$, one is free to choose two parameters, e.g., E_0 and θ_f, whereas θ_i then must be adjusted in order to obtain the desired $Q_{\parallel}$. The search for optimum intensities in this two-parameter field should be performed on a relatively fine grid, since even 5-eV changes in energy can give rise to substantial variations in intensity. In the case studied here, we have varied the impact energy in 5-eV steps for various θ_f, with θ_i adjusted to stay on the $\bar{X}$ point of the surface Brillouin zone. Once a high cross section for a particular mode was achieved, the angle of incidence θ_i was varied to probe other values of $Q_{\parallel}$. This procedure was found to be sufficient to measure the dispersion of individual branches throughout the Brillouin zone, at least for some impact energies. Spectra were recorded with an energy resolution of 60 cm^{-1}. Data were sampled at 5-cm^{-1} intervals with a total sampling time of 10—20 sec/channel. A typical number of counts was 50—300 per channel in the loss peaks. Our sample spectra presented in the next section display unsmoothed raw data. Peak positions were identified by a smoothing routine, followed by a program which identifies peaks and peak positions from mathematical properties of Gaussians. In order to minimize multiphonon scattering, the sample temperature was held at 120 K. No significant changes in the frequencies were observed between 120 K and room temperature.

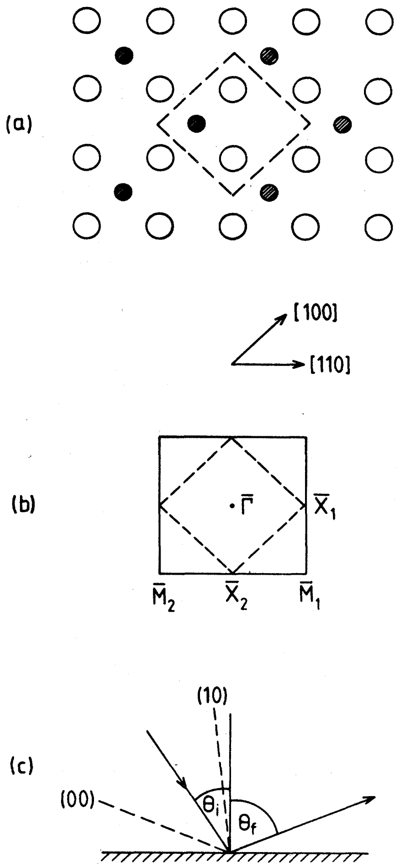

FIG. 1. (a) The $c(2\times2)$ overlayer on the Ni(100) surface with the two-dimensional unit cell (dashed line). Hatched atoms represent sulfur. (b) Surface Brillouin zone for the $c(2\times2)$ structure (dashed line) and the clean substrate surface (solid line). The notation in the Brillouin zone refers to the clean surface. (c) Scattering geometry: The scattering plane is aligned with the surface normal and the $\bar{\Gamma}-\bar{X}$ ([110]) direction.

III. EXPERIMENTAL RESULTS

In this section we present a few spectra selected to demonstrate particular aspects of the electron-phonon scattering. The features in these spectra are used to obtain the dispersion curve, which we also present. We begin with an example which illustrates, very strikingly, the rapid oscillations of the scattering cross section as a function of energy, and also the specificity of the cross section to the polarization of the modes. In Fig. 2 we display two spectra obtained with the same position of the analyzer. The impact energy E_0 was 175 and 170 eV, respectively, and the angle of incidence was adjusted so that ζ is equal

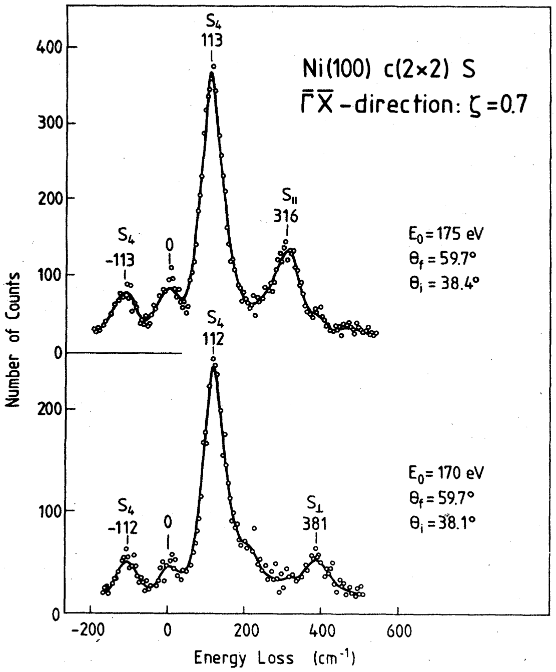

FIG. 2. Spectra for the reduced wave vector $\zeta=0.7$ ($\zeta=Q_{\|}/1.26$ Å^{-1}) taken at impact energies differing by only 5 eV. For 170 eV the spectrum displays a loss peak due to the perpendicularly polarized branch of the sulfur modes ($S_{\perp}$), whereas at 175 eV the loss peak appearing at 316 cm^{-1} represents the parallel branch ($S_{\|}$).

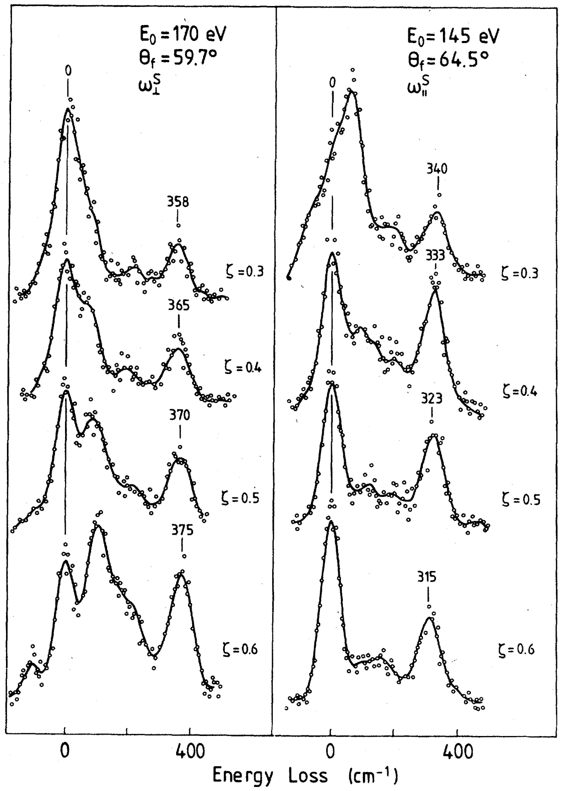

FIG. 3. Series of spectra obtained at 170 and 145 eV for ζ ranging from 0.3 to 0.6. The spectra demonstrate that at these particular energies one remains selectively sensitive to one of the sulfur-associated dispersion branches, while the angle of incidence is varied to obtain different $Q_{\|}$.

to 0.7 in each case [$\zeta=Q_{\|}/Q_{\|}(\bar{X})$, $Q_{\|}(\bar{X})=1.26$ Å^{-1}]. In both spectra, the loss peak due to the Rayleigh mode at 112 cm^{-1} (S_4 mode[16]) remains at the same intensity and energy, whereas the higher loss peak shifts from 316 to 381 cm^{-1}. Further investigation at energies above 175 eV and below 170 eV, as well as at energies in between, showed that the peaks at 316 and 381 cm^{-1} indeed represent two branches of the dispersion curves for the sulfur modes (with different polarization), and that in the energy range between 170 and 175 eV one loses the sensitivity for the one branch in exchange for the other. It has been shown in previous theoretical calculation that these strong and sharp interferences are essentially due to intralayer multiple scattering.[18] These multiple-scattering effects are also responsible for the fact that modes in which the atoms vibrate parallel with respect to the surface can be observed with electron scattering, which would otherwise be unfavorable if the simple Born approximation would hold.

While one has rather rapid oscillations in the cross sections in some regions of the scattering parameters, one also finds particular values of E_0 and θ_f, where one may vary θ_i as to obtain different $\mathbf{Q}_{\|}$, and yet have a nearly constant cross section for one particular dispersion branch. Two examples are shown in Fig. 3 for $\zeta=0.3$–0.6. The one series obtained at $E_0=170$ eV and $\theta_f=59.7°$ shows the sulfur-associated mode (which will be identified as being primarily perpendicularly polarized in our theoretical analysis) and its dispersion. The other series, obtained at 145 eV and $\theta_f=64.5°$, shows the second ("parallel") branch of sulfur. The fact that there is no significant mixing of the two modes is easily seen from the width of the peaks. A summary of the peak positions obtained in this and other series of measurement is given in Fig. 4. The solid and dashed lines are dispersion curves calculated from our lattice-dynamical model (Sec. V). The shaded area indicates the range of bulk nickel modes. The two sulfur-associated branches above the bulk modes are indicated by squares and triangles. The data point at $\bar{\Gamma}$ agrees with previous[13] measurements and represents the frequency of the vertical mode of sulfur. The observation of the parallel sulfur mode at $\bar{\Gamma}$ is forbidden by the selection rule in both dipole and impact scattering.[15] The Rayleigh mode (S_4 mode) is indicated by crosses. As in previous experiments on the clean surface,[18] we have been able to find the S_6 mode which occurs in the bulk gap near $\bar{X}$. At $\bar{X}$ the S_6 mode is polarized parallel to the surface[16] and coupled to the vertical motion of the sulfur overlayer. In addition to the data points representing genuine surface modes, we have also indicated the position of other peaks which appeared as sharp and significant features in the spectra. These peaks represent resonances (see Sec. V). Their position will also prove to be important for the interpretation of the data. An example

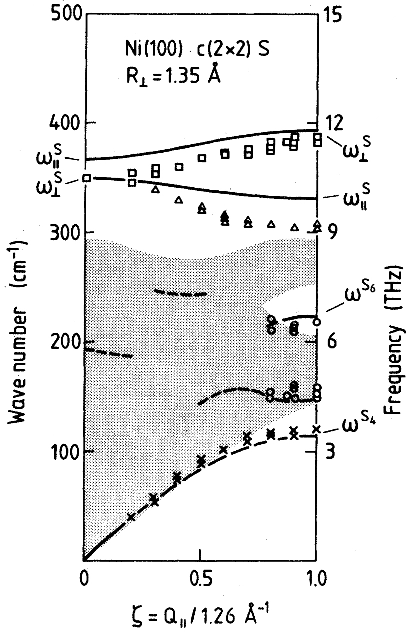

FIG. 4. Collection of data points on the dispersion curves for $c(2\times2)$ S on Ni(100). The crosses mark the Rayleigh mode (S_4 mode), the squares and triangles the sulfur-associated modes. Circles indicate the S_6 mode and resonances inside the bulk continuum, respectively. The bulk continuum is represented by the shaded area. The solid lines are dispersion curves of genuine surface modes as obtained from our lattice-dynamical model with the sulfur placed at a vertical distance $R_\perp = 1.45$ Å. The dashed lines are surface resonances (see Sec. V).

of how a surface resonance can show up in the spectrum is the peak at 153 cm^{-1} in Fig. 5.

IV. THEORETICAL CALCULATIONS

We use a lattice-dynamical model to calculate the dispersion of the adsorbate-substrate surface modes and resonances. The model and the resulting equations are identical to those for the $c(2\times2)$ overlayer of oxygen on Ni(100) and have been discussed in detail in Ref. 6, so we will not repeat them here; instead, we will mention some of the essential features of the calculation. In order to keep the calculations free from too many unknown parameters, we consider nearest-neighbor interactions between the atoms and central forces. Next-nearest-neighbor and angle-bending interactions for the adsorbate atoms are included whenever it has seemed necessary. The Fourier-transformed Green's function constructed from the eigenvectors of the displacements of the atoms is given by

$$U_{\alpha\beta}(l_z\kappa;l_z'\kappa';\mathbf{Q}_{\|},z)=\sum_s \frac{e_\alpha^{(s)}(\mathbf{Q}_{\|};l_z\kappa)\,e_\beta^{(s)}(\mathbf{Q}_{\|};l_z'\kappa')}{z^2-\omega_s^2(\mathbf{Q}_{\|})}\ , \tag{4.1}$$

where $e_\alpha^{(s)}(\mathbf{Q}_{\|};l_z\kappa)$ is the αth Cartesian component of the eigenvector for the mode s, with $\mathbf{Q}_{\|}$ the wave-vector component parallel to the surface associated with the displacement of the κth atom in the unit cell in layer l_z, $\omega_s(\mathbf{Q}_{\|})$ is the eigenfrequency, and $z=\omega+i\epsilon$ is a complex frequency. The equations of motion for these Green's functions give rise to a hierarchy connecting the displacements of the atoms in one layer to those in the layers above and below it. As expected from symmetry considerations, however, a particular type of atomic displacement in one layer couples to only a small number of combinations of displacements in the layers above and below it. For example, for the $c(2\times2)$ adsorbate overlayer on Ni(100), the motion of the adsorbate atoms perpendicular to the surface is connected to two types of motions of the atoms in the layer below it—one resulting from the vertical motion of the two nickel atoms in the unit cell (the surface unit cell as shown in Fig. 1 consists of one adsorbate atom and two substrate atoms), and the other from the motion of these two nickel atoms parallel to the surface in mutually perpendicular directions. Symmetry arguments are also helpful in limiting the types of adsorbate-substrate displacements that will contribute to the electron-energy-loss data. Thus, as discussed earlier, the S_1 mode will not appear in the dispersion measurement along the $\overline{\Gamma}$—$\overline{X}$ direction of the crystal as long as the scattering plane is aligned with the sagittal plane, since S_1 is odd with respect to this mirror plane. It is also clear that this mode does not couple to the even modes of the adsorbate atoms. We have therefore not shown the calculated dispersion of the S_1 mode in Fig. 4.

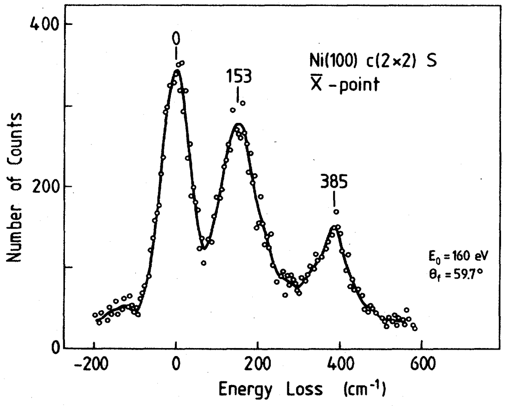

FIG. 5. Sample spectrum showing the surface resonance at 153 cm^{-1} and the vertical sulfur mode at 385 cm^{-1}.

To return to the hierarchy of Green's functions that emerge from the equation of motion, we solve the equations for the atomic displacements in the bulk of the crystal by invoking an exponential ansatz. We are then left with a set of equations for the atomic displacements in the surface layers. The number of layers contributing to this set of equations is determined by whether or not we want to be able to vary the interlayer force constant at the surface from the value in the bulk crystal. We have seen that for the clean Ni(100) surface, and also for that covered by an oxygen overlayer, the force constant between the first- and second-layer nickel atoms varies markedly from its value in the bulk. For sulfur overlayers we would also like to retain this flexibility in order to obtain a better fit to the data. Consequently, we have to treat the second-layer nickel atoms as distinct from the bulk layers, while allowing the third layer down to resemble the bulk. As in the case of the $c(2\times2)$ oxygen overlayer, this means there are a total of twelve equations in the set for the surface layers which are solved exactly, using standard computer programs.

V. COMPARISON OF THEORETICAL RESULTS WITH EXPERIMENTAL DATA

In this section we present an analysis of the theoretical results in the context of the experimental data which were presented earlier. As discussed in Ref. 19, the quantity that is relevant to the electron-energy-loss spectrum is the phonon spectral density, which is defined from the Green's function for the atomic displacements such that

$$\rho_{\alpha\beta}(l_z\kappa;l_z'\kappa';\mathbf{Q}_{\parallel}\omega)=\frac{i\omega}{\pi}[U_{\alpha\beta}(l_z\kappa;l_z'\kappa';\mathbf{Q}_{\parallel},\omega+i\epsilon)-U_{\alpha\beta}(l_z\kappa;l_z'\kappa';\mathbf{Q}_{\parallel},\omega-i\epsilon)]\ . \quad (5.1)$$

The diagonal elements of the spectral densities for the various atoms in different layers represent the squares of the amplitudes of the atoms for individual branches and $Q_{\parallel}$ values. Peaks in the spectral densities should therefore appear at frequencies at which an incident electron suffers an energy loss or gain. One should remember, however, that an actual loss spectrum will differ from the spectral densities, since the cross section for electron scattering depends on intralayer and interlayer interference processes, which are a strong function of the scattering parameters. Spectral densities therefore predict where loss peaks may appear, given that one has appropriate scattering parameters. The fact that electron scattering can be made sensitive to particular parts of the spectral densities is important since it permits a comparatively precise analysis of the dispersion curves despite the low resolution.

Our procedure for making contact with the experimental data is to first construct the above spectral densities from the calculated Green's functions. We next plot the spectral densities for a particular $\mathbf{Q}_{\parallel}$, for the types of vibration of the adsorbate and substrate atoms that we expect to participate in the scattering processes, as a function of ω, the real part of the complex frequency. The sharpness of the features is controlled by the phenomenological damping ϵ that we have introduced in our definition of the Green's function. For small values of ϵ, features arising from surface modes or resonances appear almost like δ functions in this plot, while the bulk-phonon contributions are broader. As we increase ϵ to correspond to a more realistic situation, the surface modes and resonances appear with a finite width and the bulk mode features broaden considerably more. Two examples of spectral-density plots are shown in Fig. 6. Here the S_4 and S_6 modes appear in either spectrum as a sharp feature at 112 and 222 cm^{-1}, respectively, as do the sulfur surface modes for both perpendicular and parallel motion. The other features are the adsorbate-substrate resonances, which are broader as they lie inside the bulk band, and the coupling to bulk modes provides the extra damping. Later we will see that these modes decay rapidly as one moves away from the $\bar{X}$ point.

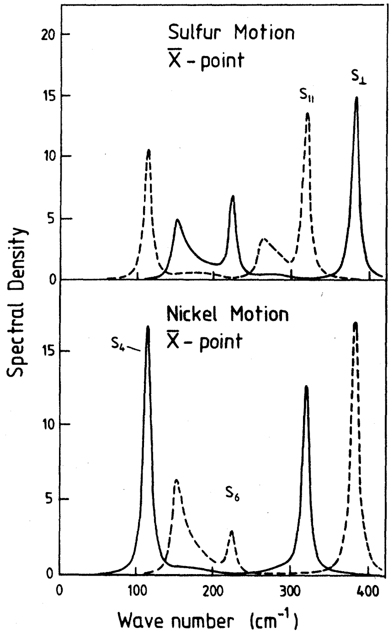

FIG. 6. Spectral densities at the $\bar{X}$ point for the sulfur atoms and first-layer nickel atoms, respectively. The solid line represents the perpendicular motion, the dotted line the parallel. At the $\bar{X}$ point the parallel motion of the sulfur atoms couples to the perpendicular motion in the first-layer nickel and vice versa.

The calculated dispersion curve for all modes is now easily obtained by following the frequency of each mode in the spectral-density plots for a range of $Q_{\parallel}$ values along a particular direction in the two-dimensional Brillouin zone. As we can see from Fig. 6 the dispersion curves can be obtained from either the sulfur or nickel spectral densities.

Before we present a comparison of the experimental data and calculated dispersion curves, we would like to discuss the parameters that enter the calculation of the Green's function from the lattice-dynamical model. As described in earlier works,^{6,19} the parameters needed are the force constants for the adsorbate-substrate interaction, the vertical distance at which the adsorbate atom sits on top of the fourfold hollow site, and the force constants for the interaction between the nickel atoms. The latter, for the bulk atoms, is obtained from a one-parameter fit to the phonon dispersion curve, which is reasonable for nickel, where deviations from Cauchy relations are small and the nearest-neighbor model works rather well. We have chosen the intralayer force constants for the first- and second-layer nickel atoms to be equal to the bulk value, while allowing the interlayer force constant k_{12} (between the first and second layers) to vary so as to give a good fit to the frequency of the Rayleigh wave (the S_4 mode) at the $\bar{X}$ point of the two-dimensional Brillouin zone, since it is then most sensitive to the variation of k_{12}. In the case of a $c(2\times2)$ overlayer of oxygen on Ni(100), it was found^6 that $k_{12}=0.3k$, where k is the force constant in the bulk crystal, gave a good fit to the dispersion of the S_4 mode along the $\bar{\Gamma}-\bar{X}$ direction, while, for the clean

Ni(100) surface, $k_{12}=1.2k$ gave a good agreement with the data along both the $\bar{\Gamma}$—$\bar{X}$ and $\bar{\Gamma}$—$\bar{M}$ directions.[3,20] We will see that with a $c(2\times2)$ overlayer of sulfur the Ni(100) surface behaves almost like the clean nickel surface, i.e., a value for k_{12} of $1.2k$ or even $1.3k$ gives a reasonably good fit to the dispersion of the Rayleigh wave.

The remaining two parameters, $R_\perp$, the vertical distance above the Ni(100) surface at which the sulfur atom sits in the fourfold hollow site, and the sulfur-nickel force constant ϕ_{10}'', are mutually coupled. It would have been best to obtain these two quantities from *ab initio* calculations. The only such calculation[21] that we are aware of assigns $R_\perp$ as 1.24 Å and the sulfur-nickel force constant as 1.26×10^5 dyn cm^{-1}. Since this estimate of $R_\perp$ is considerably lower than the recently measured[9–12] values of about 1.35 Å, we have proceeded differently in our choice of the two parameters. We have explored the effect of variation of $R_\perp$, between 1.3—1.5 Å, on the dispersion of the modes. For each choice of $R_\perp$, we have extracted the sulfur-nickel coupling constant from a fit to the experimentally observed value of 350 cm^{-1} for the frequency of $\omega_\perp^S$ at the $\bar{\Gamma}$ point. The combination of k_{12}, $R_\perp$, and nickel-sulfur force constant that gives the best fit to the experimentally observed dispersion of all the modes determines the quality of the match between theory and experiment. There are no free parameters in the theory. We now proceed to study the effect of variation of $R_\perp$ on the dispersion curves.

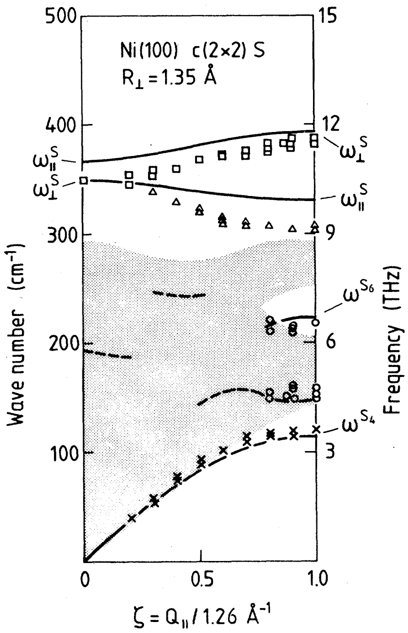

FIG. 7. Dispersion of the $c(2\times2)$ S on Ni(100) surface modes and resonances for a choice of $R_\perp=1.35$ Å, $k_{12}=1.2k$, and $\phi_{10}''=1.13\times10^5$ dyn cm^{-1}. The solid lines are the calculated dispersion of the surface modes, the dashed lines those of the adsorbate-induced resonances. The data points are as described in Fig. 4.

A. $R_\perp=1.35$ Å

In Fig. 7 we present the match to the data with theoretical curves (solid lines) obtained with $R_\perp=1.35$ Å, $k_{12}=1.2k$, and $\phi_{10}''=1.13\times10^5$ dyn cm^{-1}. The lowest-lying line is the Rayleigh wave (S_4 mode), whose fit with $k_{12}=1.2k$ is reasonably good, although $k_{12}=1.3k$ would have been even better. We shall return to this later. Here we shall mainly focus on the dispersion of the sulfur modes for vibrations perpendicular and parallel to the surface. These are the two top-lying modes in the figure, with the interesting feature that the upper and lower branches change polarity as one goes from the $\bar{\Gamma}$ to the $\bar{X}$ point of the two-dimensional Brillouin zone. To illustrate how the polarity of the modes changes, in Fig. 8 we present a series of spectral-density plots for the perpendicular (solid curve) and parallel (dashed curve) motion of the sulfur atoms at successive points on the line from $\bar{\Gamma}$ to $\bar{X}$, for the set of parameters given above. One sees that the lower-frequency sulfur dispersion branch, which is polarized perpendicularly at $\bar{\Gamma}$, assumes a parallel component as one moves along $\bar{\Gamma}$—$\bar{X}$, and eventually turns into a pure parallel mode at $\bar{X}$. The crossover point where the two sulfur dispersion branches have a nearly equal contribution of parallel and perpendicular motion is near $\zeta=0.4$. We find this theoretical result difficult to reconcile with the experimental data as presented in Fig. 3. There we have seen that, by using different impact energies, it was possible to generate series of spectra which displayed only a contribution from either the upper or lower branch. This particular sensitivity to either branch stems from constructive and destructive interference in the multiple (mostly intralayer) scattering.[17] Although no dynamical analysis of the inelastic cross sections exists for the $c(2\times2)$ sulfur overlayer, one would tend to assume that the selectivity to one branch cannot be preserved when the modes have a crossover in polarization. Thus, if the polarization crossover were to occur, one would expect to see a broad loss peak centered at a frequency between the two branches in both series of spectra in Fig. 3 as the value of $Q_\parallel$ approaches the crossover point. Instead, we see (in Fig. 3) that the loss peaks due to the sulfur modes stay on separate branches for $\zeta=0.3$—0.6. We therefore conclude that the case for the polarization crossover of the modes cannot be defended on experimental grounds. We also note that the fit of the dispersion curve in Fig. 6 is rather poor, which in itself is a sufficiently strong reason to proceed to another choice of parameters.

As we have stated before, the parameter set used here was not arbitrarily chosen. In particular, $R_\perp=1.35$ Å was taken from independent structure analyses. Before proceeding with the discussion of our lattice-dynamical analysis with different $R_\perp$, we explore the effect of a more general force field on the dispersion curve. It is clear from the above argument that mode mixing along the $\bar{\Gamma}$—$\bar{X}$ direction is not realistic. This mixing would not have occurred if at $\bar{\Gamma}$ the parallel mode were to lie below the perpendicular one. In order to facilitate this, one may generalize the force field in two ways. One way would be to introduce angle-bending forces for the Ni—S—Ni bond angle. The additional terms which then enter the equations of motion are contained in Ref. 6. We have tested

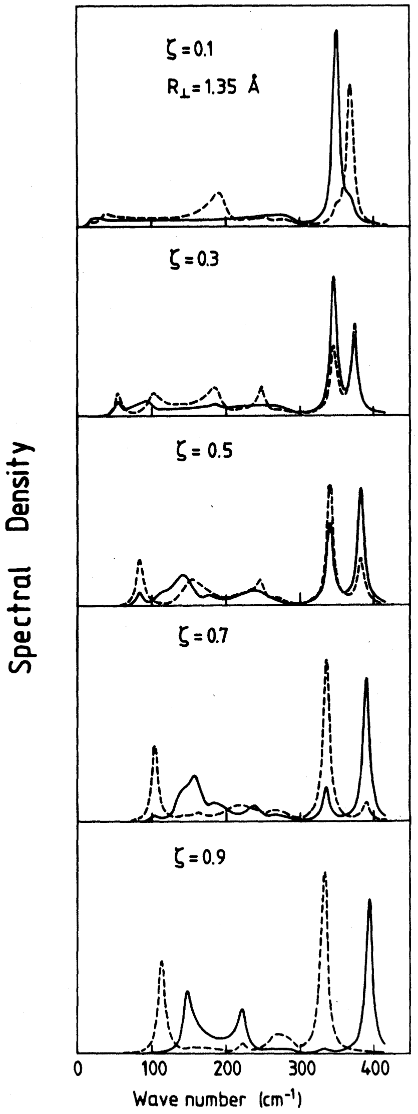

FIG. 8. Spectral-density plots for the sulfur atoms with $R_\perp=1.35$ Å, $k_{12}=1.2k$, and $\phi''_{10}=1.13\times10^5$ dyn cm^{-1} for various values of $\zeta=Q_\parallel/Q_\parallel(\bar{X})$, along the $\bar{\Gamma}-\bar{X}$ direction. The motion of sulfur perpendicular to the surface is denoted by solid lines, that for motion parallel to the surface by dashed lines.

the effect of angle-bending forces for the sulfur modes and found that, while it is possible to generate branches which essentially retain their polarization throughout the $\bar{\Gamma}-\bar{X}$ direction, with the lower branch being the parallel mode, the calculated dispersion of the modes is much flatter than experimentally observed. We therefore conclude that the inclusion of angle-bending interactions does not lead to a reasonable agreement between theory and experiment.

We next tested the inclusion of second-nearest-neighbor coupling between the sulfur and the second-layer nickel atom directly below it. With this term included, a satisfactory fit to the sulfur dispersion was achieved for a choice of sulfur—second-neighbor-nickel force constant of one-tenth of the sulfur—nearest-neighbor-nickel force constant. However, the resonance at $\bar{X}$ near 150 cm^{-1}, which involves a perpendicular motion of sulfur and the second-layer nickel atoms (and a parallel motion of the first-layer nickel atoms), is then shifted upwards to $\sim$200 cm^{-1}. Experimentally, we have found the resonance at 150 cm^{-1} to be a rather prominent feature for many choices of the scattering parameters (Fig. 5). We therefore believe that the coupling of sulfur to the second-neighbor nickel atom is not significant. Furthermore, the inclusion of a second-nearest-neighbor coupling as described above, yet

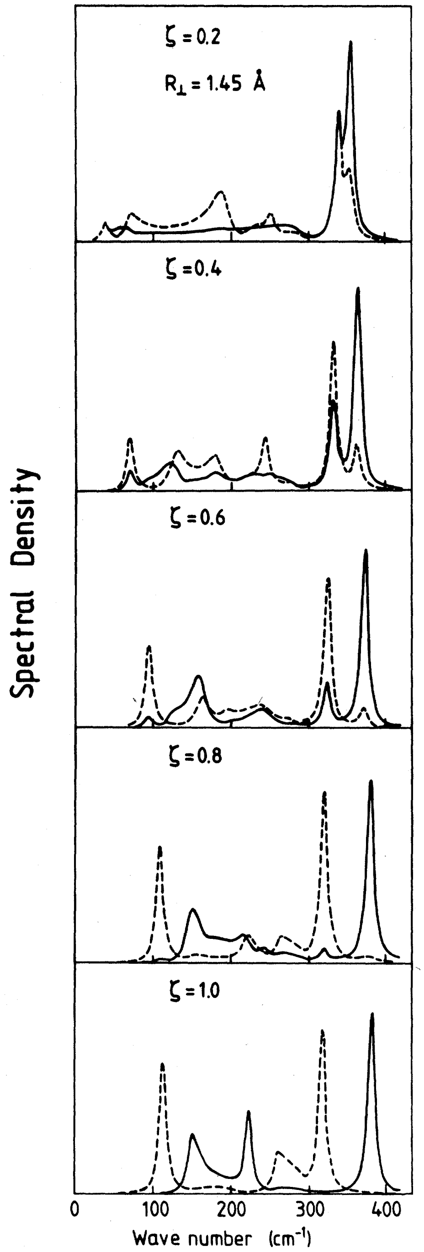

FIG. 9. Spectral-density plots for the sulfur atoms with $R_\perp=1.45$ Å, $k_{12}=1.2k$, and $\phi''_{10}=9.97\times10^4$ dyn cm^{-1} for various values of $\zeta=Q_\parallel/Q_\parallel(\bar{X})$, along the $\bar{\Gamma}-\bar{X}$ direction. The motion of sulfur perpendicular to the surface is denoted by solid lines, that for motion parallel to the surface by dashed lines.

disregarding coupling between the sulfur atoms, is hardly justified. Lateral coupling between the sulfur atoms will, however, pull the frequency of the sulfur parallel mode further up at $\bar{X}$, in further disagreement with the data.

We are therefore led to conclude that no simple extension of the force field provides a satisfactory fit to the data as long as the vertical distance of the sulfur layer is retained at $R_{\perp}=1.35$ Å.

B. $R_{\perp}=1.45$ Å

The distance required to obtain a good match with the sulfur dispersion curves is $R_{\perp}=1.45$ Å. We take $k_{12}=1.2k$ as before, and obtain $\phi_{10}''=9.97\times10^4$ dyn cm^{-1} from the frequency of the vertical sulfur mode at $\bar{\Gamma}$. With these parameters, a good match to the experimental data is achieved (Fig. 4). No angle-bending terms or next-nearest-neighbor interactions need to be included. In Fig. 9 we display the spectral densities for sulfur, with this set of parameters for a few selected points in the Brillouin zone. As we can see, the crossover of the polarization of the sulfur modes is now removed. The upper and the lower branches are essentially perpendicular and parallel, respectively, although some mixing of the polarization still occurs when the frequencies of the two branches become close at $\bar{\Gamma}$. The spectral densities in Fig. 9 also reproduce very nicely the S_6 mode and the resonance near $\bar{X}$ which appear in the data. As one moves away from $\bar{X}$, the resonance becomes broader and less intense. This is in agreement with our data, insofar as no prominent peaks have been found for $\zeta<0.8$ in this frequency range. In a more systematic search for optimum scattering conditions, one might find some of the resonances in other parts of the Brillouin zone as well.[22]

VI. DISCUSSION

The comparison between theory and experiment indicates that the sulfur atoms are placed at a vertical distance $R_{\perp}\approx1.45$ Å. It is difficult to suggest an error margin for this value. Yet, according to our analysis, the vertical distance should not be much smaller for a reasonable agreement between theory and experiment. The vertical distance can be converted into a bond distance for the Ni—S bond since for the $c(2\times2)$ structure no lateral movements of the nickel surface atoms are permitted [otherwise the structure would not remain $c(2\times2)$]. The resulting bond distance of 2.28 Å for the Ni—S bond is in good agreement with the Ni—S bond distance in bulk compounds (Ni_3S_2, 2.28 Å; NiS, 2.38 Å; NiS_2, 2.34 and 2.42 Å; see Ref. 8 and references therein). On the other hand, most of the structure-sensitive experimental techniques which have been applied to the $c(2\times2)$ S on Ni(100) surface have determined a slightly smaller vertical distance and bond length. Among these techniques, EXAFS is generally accepted to be the most accurate. According to the surface EXAFS analysis,[9] the Ni—S bond length on the $c(2\times2)$S on Ni(100) surface is (2.23 ± 0.02) Å, which yields a vertical distance of (1.37 ± 0.03) Å. Thus, the vertical distance from our vibrational analysis is outside the error margin estimated by Brennan *et al.* It is conceivable that the systematic error in the procedure of analyzing EXAFS data is somewhat larger than that quoted, so that the two results could be considered to be consistent. An alternative explanation for the discrepancy could probably also be found in the effects of anharmonicity on the vibrational analysis. As we have seen, the vertical distance is essentially determined from the frequency ratio of the vertical and parallel sulfur mode. Recent total-energy calculations for oxygen on nickel using an approximate effective-medium model[23] suggest that anharmonic terms in the potential are larger for a motion parallel to the surface than for the motion perpendicular to it. Qualitatively, this is easy to understand: Suppose one moves a sulfur atom parallel to the surface out of the fourfold hollow site across the bridging site into the next hollow site; then the sulfur must overcome the activation energy of diffusion, which is always significantly lower than the activation barrier for removing an atom from the surface along a trajectory normal to the surface. Anharmonic terms in the sulfur-nickel potential should therefore be larger for the parallel motion. This would reduce the transition energy from the ground state to the first-excited state (which is the quantity measured experimentally) for the parallel motion, while the effect should be less for the vertical motion. This could bring the parallel sulfur branch below the vertical branch, even for vertical distances $R_{\perp}$ smaller than 1.45 Å. No estimate with regard to the magnitude of the effect can be made at present.

A final word regarding the fit between the theory and the experiment concerns the choice of $k_{12}=1.2k$. It is clear from the frequency of the S_4 mode at $\bar{X}$ that a slightly higher value of k_{12} would have given a better fit, implying an even stronger bonding between the first- and second-layer nickel atoms than for the clean (100) surface. We have refrained from doing that because the nearest-neighbor interaction model does have its limitations, and we should not expect a perfect fit.

ACKNOWLEDGMENTS

The assistance of D. Bruchmann and U. Marx is appreciated. One of us (M.R.) wishes to thank the Centro Nazionale delle Richerche of Italy for support. The research of one of us (T.S.R.) was partially supported by the National Science Foundation under Grant No. DMR-84-02850. We also acknowledge travel support from the North Atlantic Treaty Organization under Grant No. 075/84.

---

*Permanent address: Dipartimento di Fisica, Università degli Studi di Genova, Via Dodecanneso 33, I-16100 Genova, Italy.

[1] G. Brusdeylins, R. B. Doak, and J. P. Toennies, Phys. Rev. Lett. **46**, 1138 (1980); G. Brusdeylins, R. B. Doak, and J. P. Toennies, Phys. Rev. B **27**, 3662 (1983).

[2] J. P. Toennies, J. Vac. Sci. Technol. A **2**, 1055 (1984).

[3] S. Lehwald, J. M. Szeftel, H. Ibach, T. S. Rahman, and D. L. Mills, Phys. Rev. Lett. **50**, 518 (1983).

[4] J. M. Szeftel, S. Lehwald, H. Ibach, T. S. Rahman, J. E. Black, and D. L. Mills, Phys. Rev. Lett. **51**, 268 (1983).

[5] H. Ibach, in Proceedings of the Vth International Conference on Solid Surfaces, Madrid, 1983 (unpublished).

[6] T. S. Rahman, D. L. Mills, J. E. Black, J. M. Szeftel, S. Lehwald, and H. Ibach, Phys. Rev. B **30**, 589 (1984).

[7] J. W. M. Frenken, J. F. van der Veen, and G. Allan, Phys. Rev. Lett. **51**, 1876 (1983).

[8] J. E. Demuth, D. W. Jepsen, and P. M. Marcus, Phys. Rev. Lett. **31**, 540 (1973).

[9] S. Brennan, J. Stöhr, and R. Jaeger, Phys. Rev. B **24**, 4871 (1981).

[10] D. H. Rosenblatt, J. G. Tobin, M. G. Mason, R. F. Davis, D. A. Shirley, C. H. Li, and S. Y. Tong, Phys. Rev. B **23**, 3828 (1981).

[11] J. J. Barton, C. C. Bahr, Z. Hussain, S. W. Robey, J. G. Tobin, L. E. Klebanoff, and D. A. Shirley, Phys. Rev. Lett. **51**, 272 (1983).

[12] P. J. Orders, B. Sinković, C. S. Fadley, R. Trehan, Z. Hussain, and J. Lecante, Phys. Rev. B **30**, 1838 (1984).

[13] S. Andersson, Surf. Sci. **79**, 385 (1979).

[14] S. Lehwald and H. Ibach, in *Vibrations at Surfaces,* edited by R. Caudano, J. M. Gilles, and A. A. Lucas (Plenum, New York, 1982), p. 137.

[15] For a general discussion, see H. Ibach and D. L. Mills, *Electron Spectroscopy and Surface Vibrations* (Academic, New York, 1982).

[16] R. E. Allen, G. P. Alldredge, and F. W. de Wette, Phys. Rev. B **4**, 1661 (1971).

[17] S. Y. Tong, C. H. Li, and D. L. Mills, Phys. Rev. Lett. **44**, 407 (1980); C. H. Li, S. Y. Tong, and D. L. Mills, Phys. Rev. B **21**, 3057 (1980); S. Y. Tong, C. H. Li, and D. L. Mills, *ibid.* **24**, 806 (1981).

[18] Mu-Liang Xu, B. M. Hall, S. Y. Tong, M. Rocca, H. Ibach, S. Lehwald, and J. E. Black (unpublished).

[19] T. S. Rahman, J. E. Black, and D. L. Mills, Phys. Rev. B **25**, 883 (1982).

[20] M. Rocca, S. Lehwald, H. Ibach, and T. S. Rahman, Surf. Sci. Lett. **138**, L123 (1984).

[21] T. Upton and W. A. Goddard, Phys. Rev. Lett. **46**, 1635 (1981).

[22] For the clean Ni(100) surface, we have covered a wider range of scattering parameters and have found most of the resonances as indicated by the spectral densities calculated for the clean surface.

[23] B. Chakraborty, S. Holloway, and J. K. Nørskov (unpublished).